

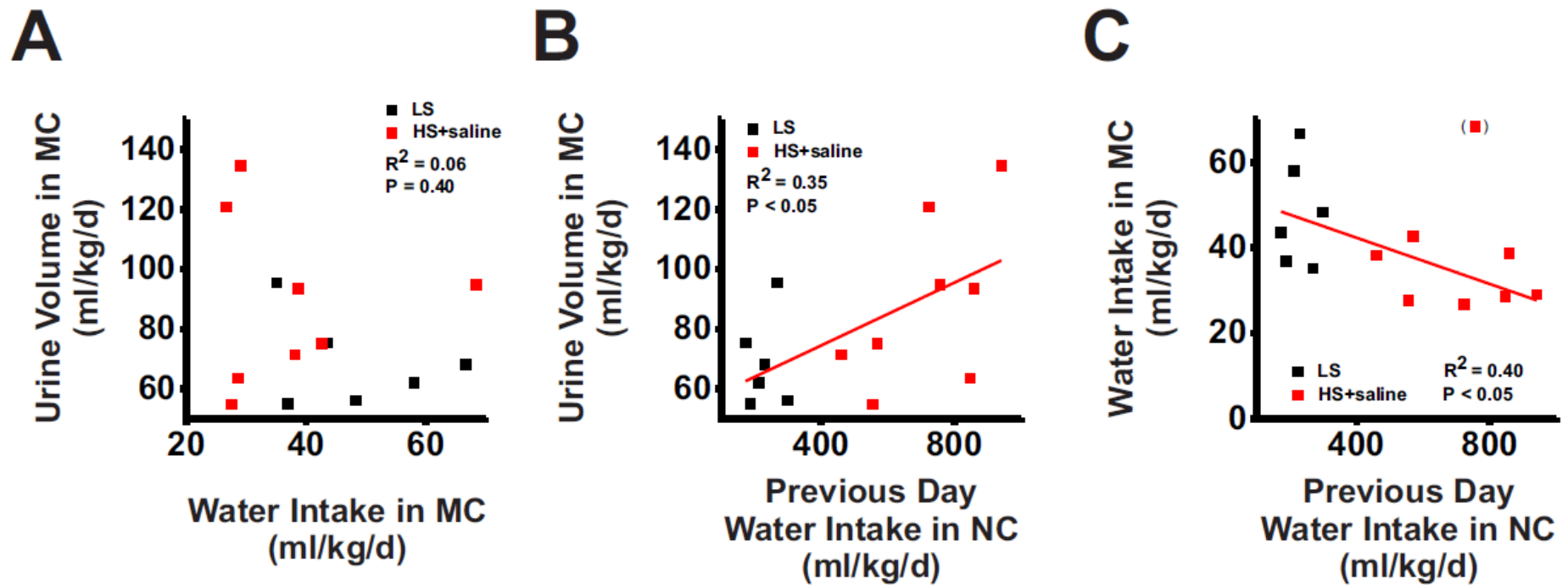
High-salt intake reprioritizes osmolyte and energy metabolism for body fluid conservation

Kento Kitada, Steffen Daub, Yahua Zhang, Janet D. Klein, Daisuke Nakano, Tetyana Pedchenko, Louise Lantier, Lauren M. LaRocque, Adriana Marton, Patrick Neubert, Agnes Schröder, Natalia Rakova, Jonathan Jantsch, Anna E. Dikalova, Sergey I. Dikalov, David G. Harrison, Dominik N. Müller, Akira Nishiyama, Manfred Rauh, Raymond C. Harris, Friedrich C. Luft, David H. Wassermann, Jeff M. Sands, and Jens Titze

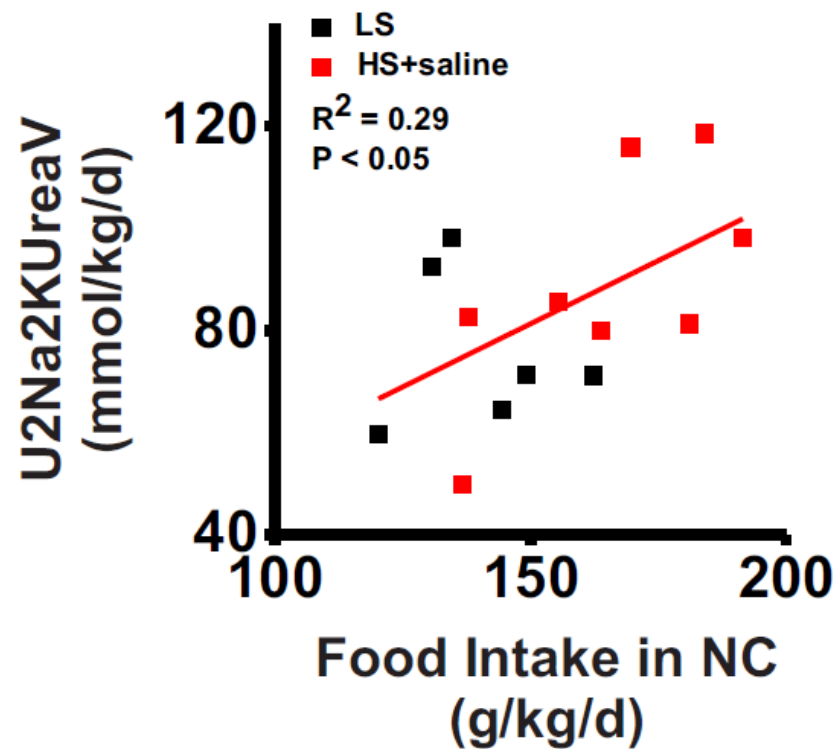
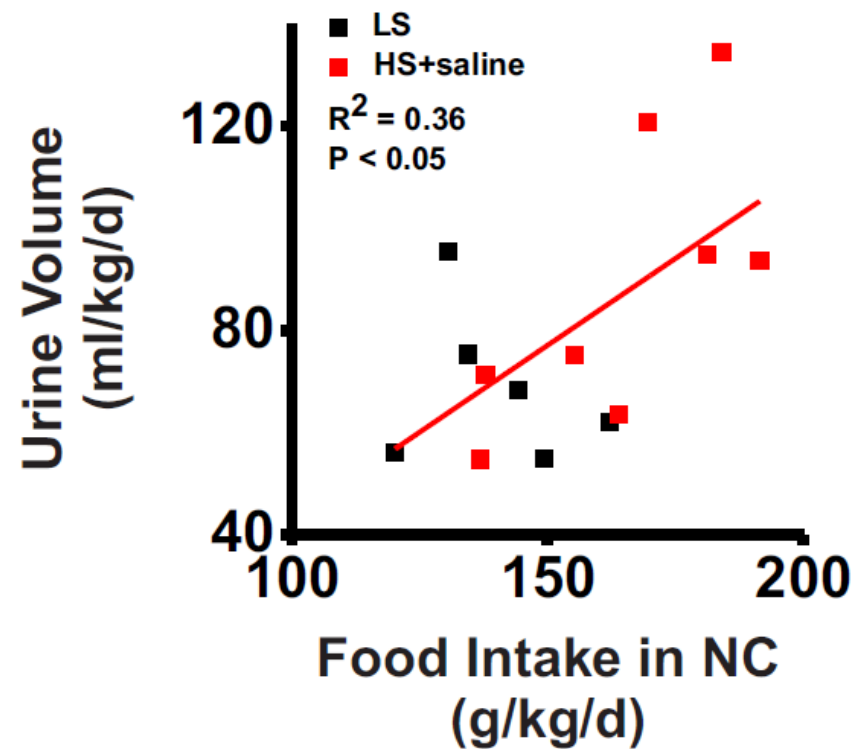
Online Supplemental Materials

Inventory:

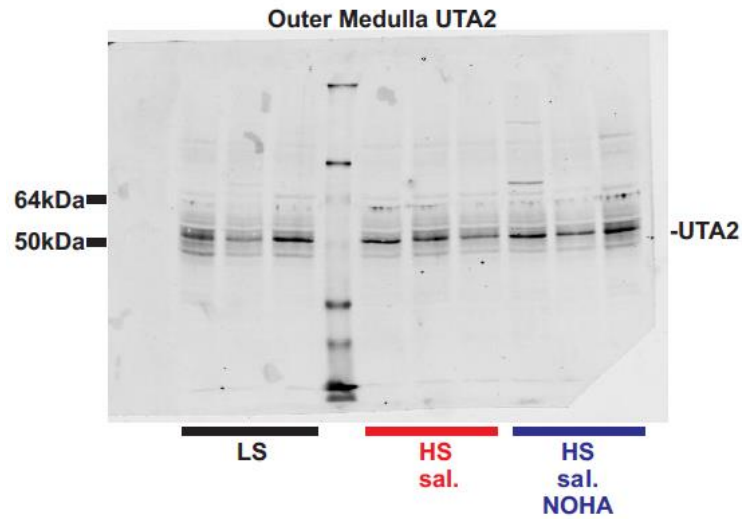
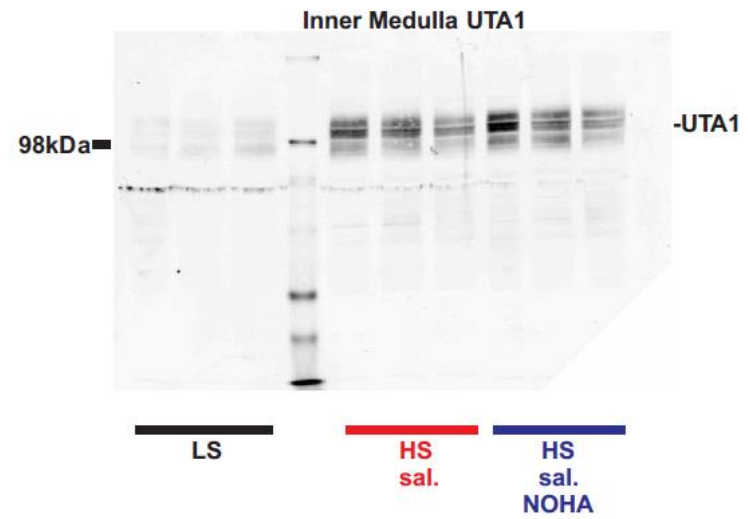
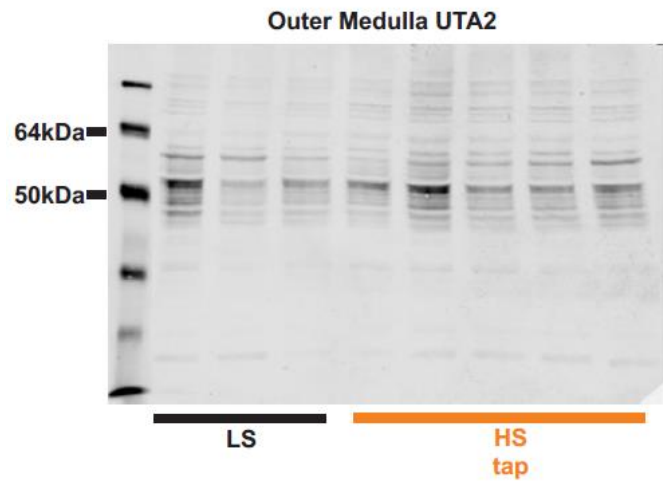
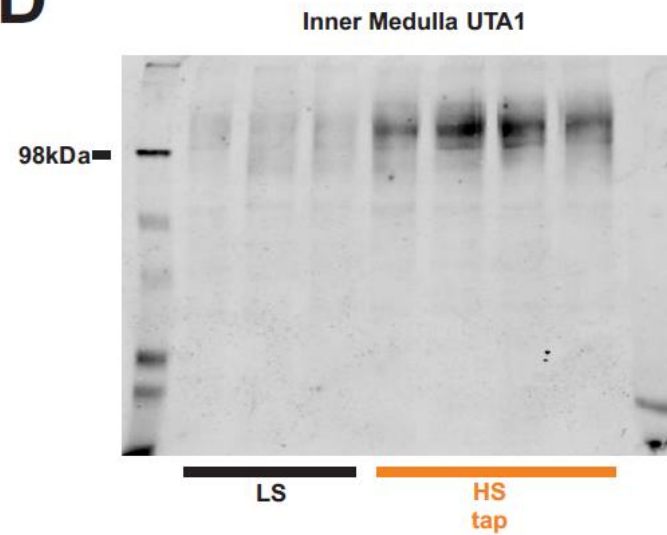
Online Supplemental Figure 1	Page 2
Online Supplemental Figure 2	Page 3
Online Supplemental Figure 3	Page 4
Online Supplemental Figure 4	Page 5
Online Supplemental Figure 5	Page 6
Online Supplemental Figure 6	Page 7
Online Supplemental Figure 7	Page 8
Online Supplemental Figure 8	Page 9
Online Supplemental Figure 9	Page 10
Online Supplemental Figure 10	Page 11
Online Supplemental Figure 11	Page 12
Online Supplemental Figure 12	Page 13
Online Supplemental Figure 13	Page 14
Online Supplemental Figure 14	Page 15
Online Supplemental Figure 15	Page 16
Online Supplemental Table 1	Page 17



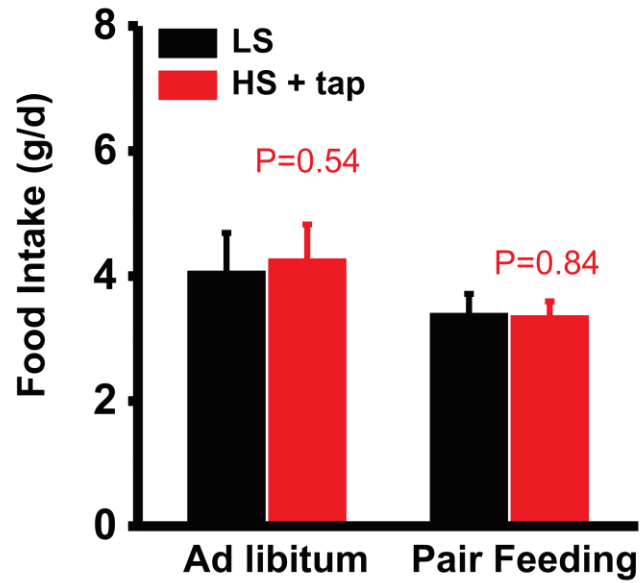
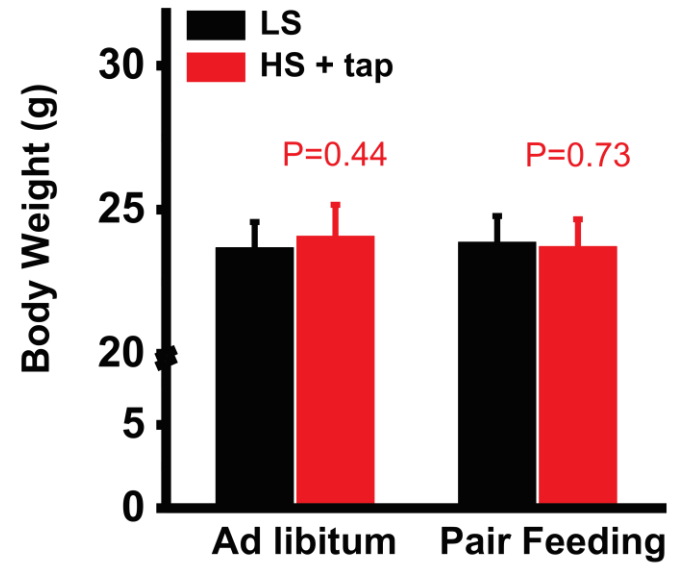
Online Supplemental Figure 1: *Time-dependent relationship between water intake and urine volume formation in mice in metabolic cages.* *Panel A.* Relationship between 24-h water intake and urine volume formation in LS (n=6) and HS+saline (n=8) mice. Water intake and urine volume was monitored while the mice were housed in the metabolic cage (MC) for urine collection. *Panel B.* Relationship between previous day water intake in the normal cage (NC) and following day urine volume generation in the MC in the same mice. *Panel C.* Relationship between previous day water intake in the NC and following day water intake in the MC in the same mice.

A**B**

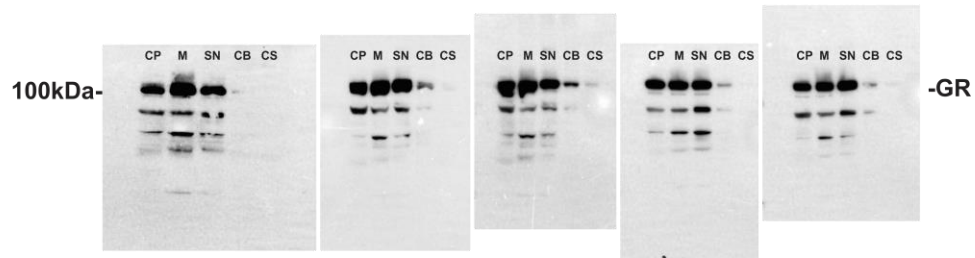
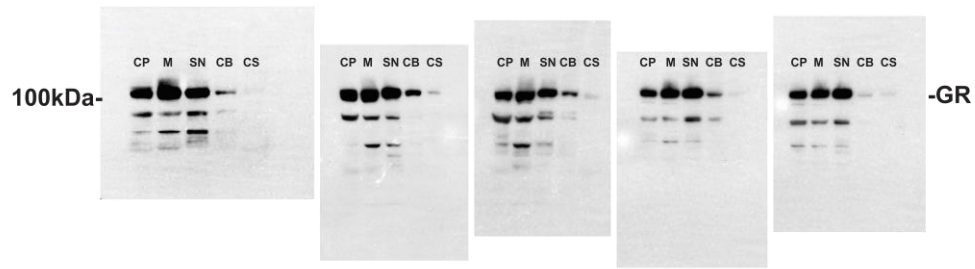
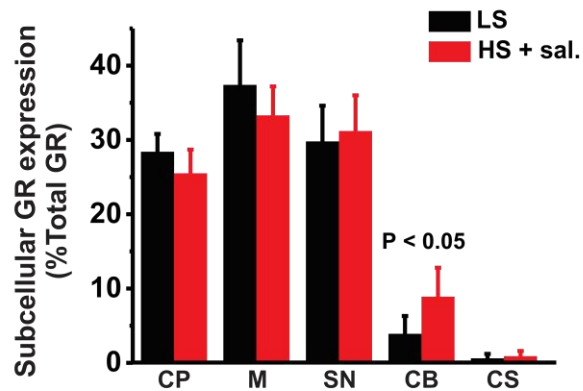
Online Supplemental Figure 2: *Time-dependent relationship between food intake and urine osmolyte and water excretion in mice in metabolic cages. Panel A.* Relationship between previous day food intake in the normal cage (NC) and following day urine 2Na^+ , 2K^+ , and urea excretion (U2Na2KUreaV) in the metabolic cage (MC) in LS (n=6) and HS+saline (n=8) mice. *Panel B.* Relationship between previous day food intake in the NC and following day urine volume formation in the MC in the same mice.

A**B****C****D**

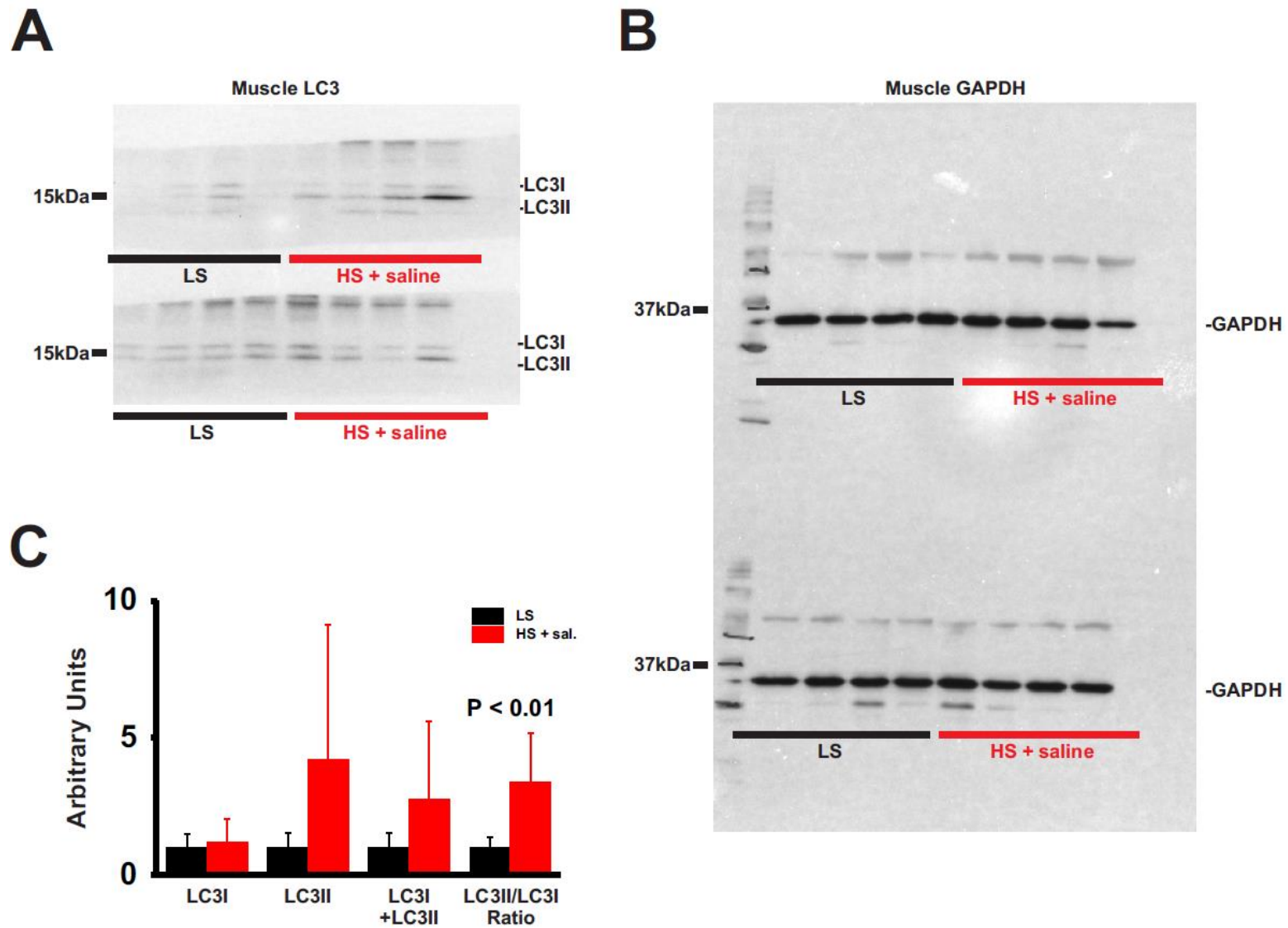
Online Supplemental Figure 3: Full western blots of urea transporter A1 (UT-A1) and A2 (UT-A2) expression in inner and outer medulla of mice with low salt (LS; n=3) or high salt diet (HS+saline; n=3, HS+tap; n=4 or 5), or in HS+saline mice with additional N- ω -Hydroxy-L-norarginine treatment (HS+saline+NOHA; n=3).

A**B**

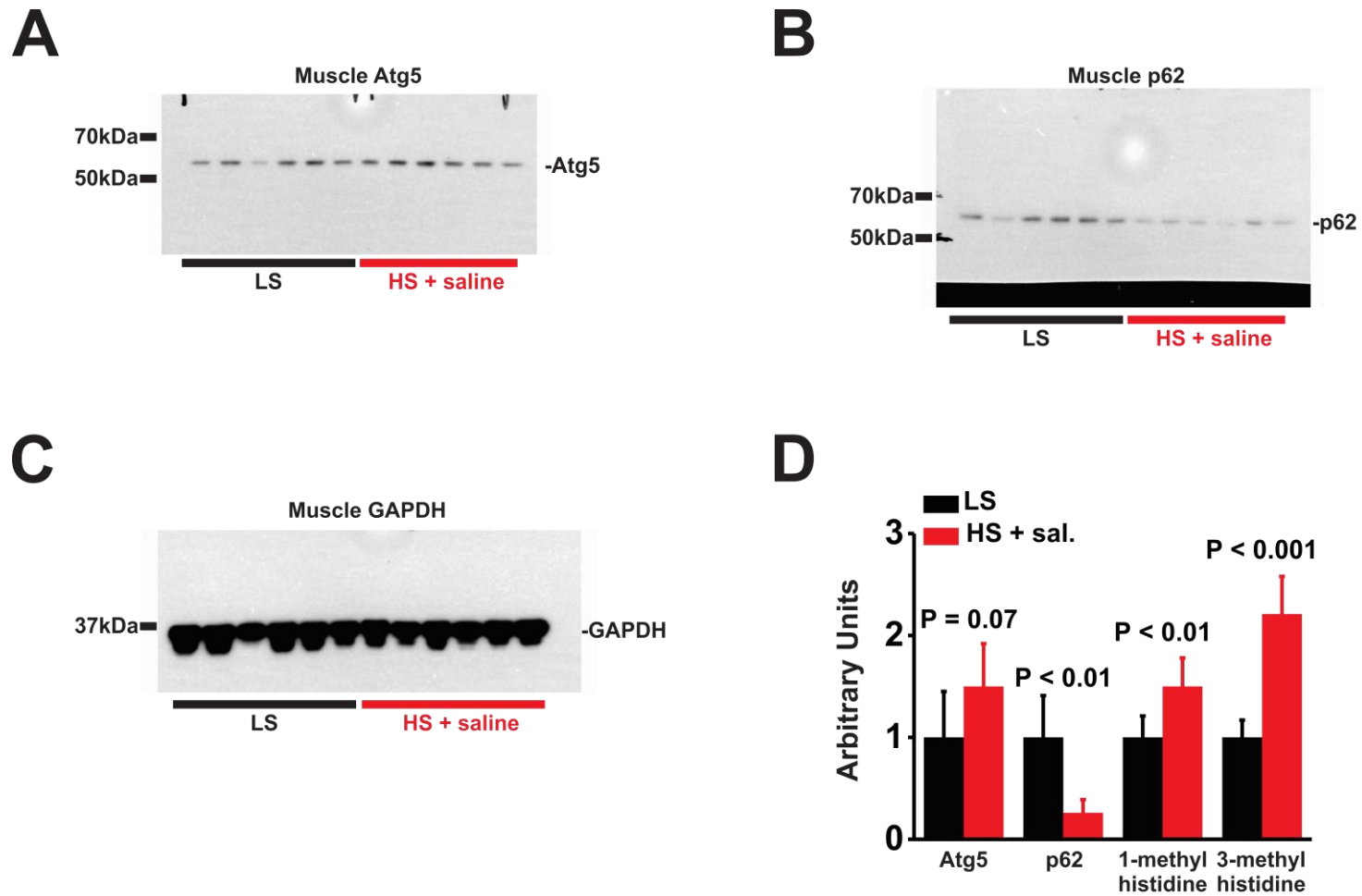
Online Supplemental Figure 4: *Food intake and body weight changes in LS (n=7) and HS+tap (n=7) mice after 4 weeks ad libitum feeding, and after the following 2 weeks of pair-feeding. Panel A. Food intake. Panel B. Body weight.*

A**LS group
Muscle subcellular GR expression****B****HS + saline group
Muscle subcellular GR expression****C**

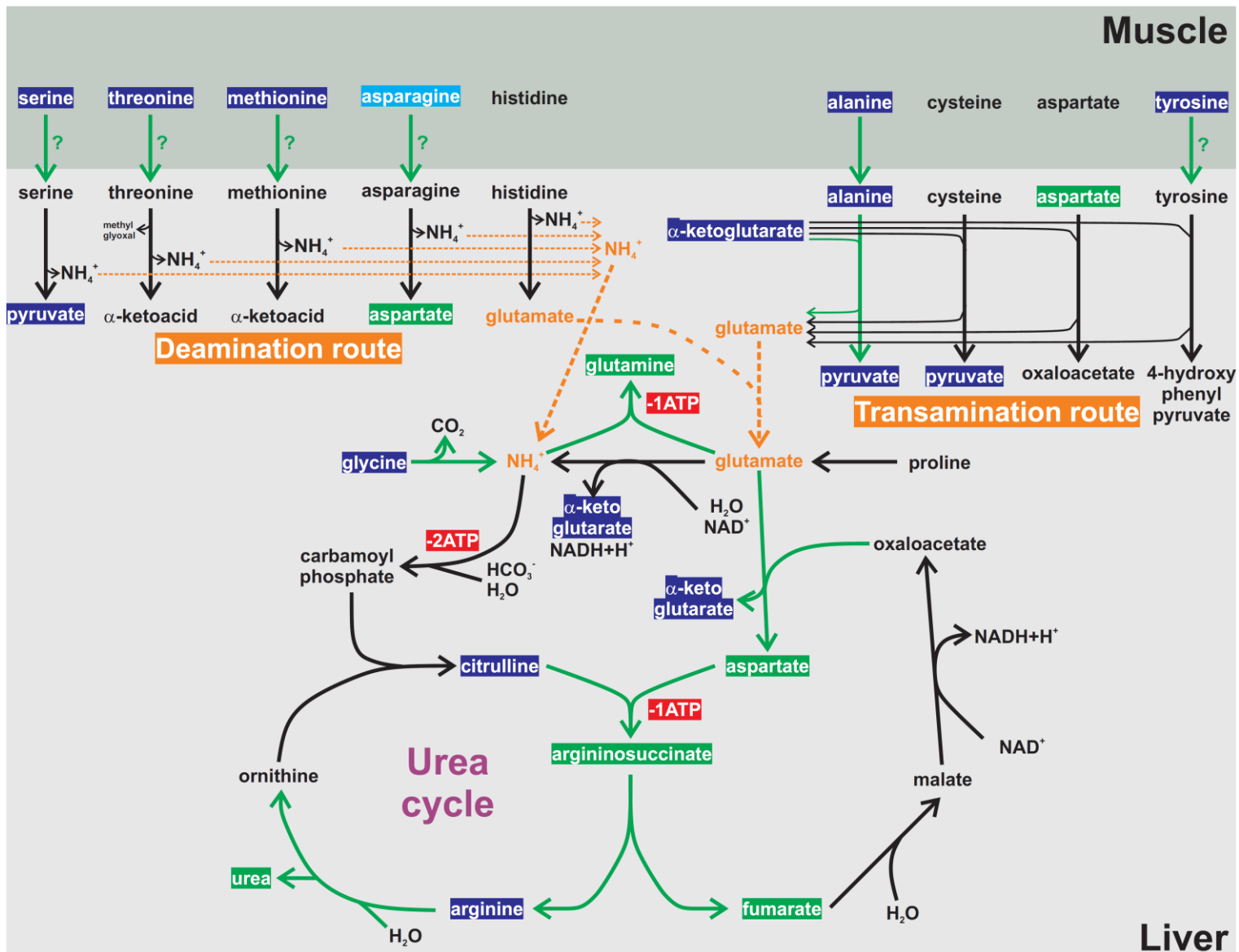
Online Supplemental Figure 5: Full western blots of glucocorticoid receptor (GR) expression in skeletal muscle of mice with low salt (LS; n=5) or high salt diet (HS+saline; n=5). *Panel A:* Full western blots for each animal analyzed in the LS group. *Panel B:* Full western blots for each animal analyzed in the HS+saline group. *Panel C:* Quantification of fractional protein expression. CP: cytoplasmic fraction, M: membrane fraction, SN: soluble nuclear fraction, CB: chromatin-bound fraction, CS: cytoskeletal fraction.



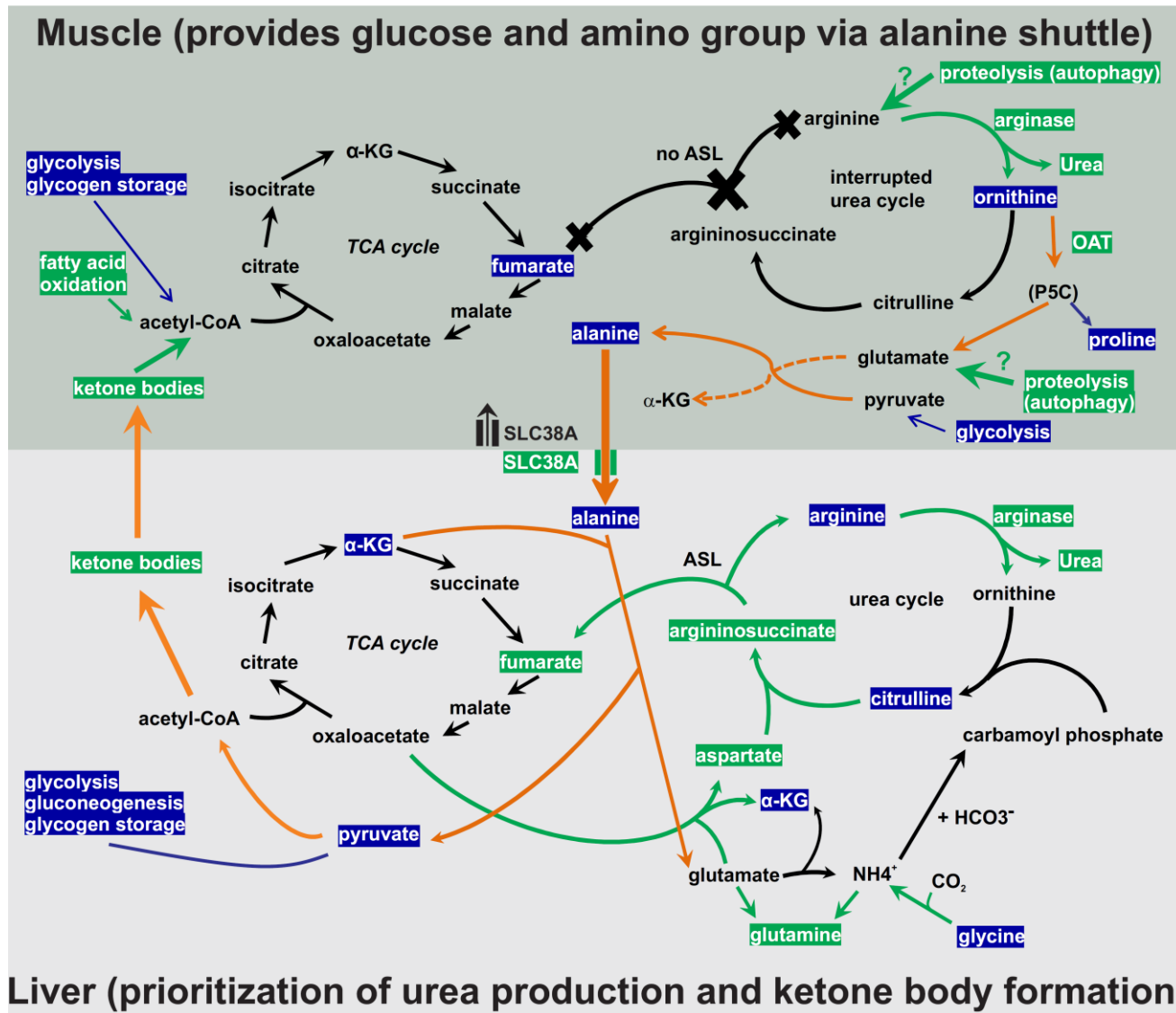
Online Supplemental Figure 6: Full western blots of LC3I and LC3II expression in skeletal muscle of mice with low-salt (LS; n=8) or high-salt diet (HS+saline; n=8). *Panel A and B:* Full western blots. *Panel C:* Quantification of LC3I and LC3II protein relative to GAPDH protein expression.



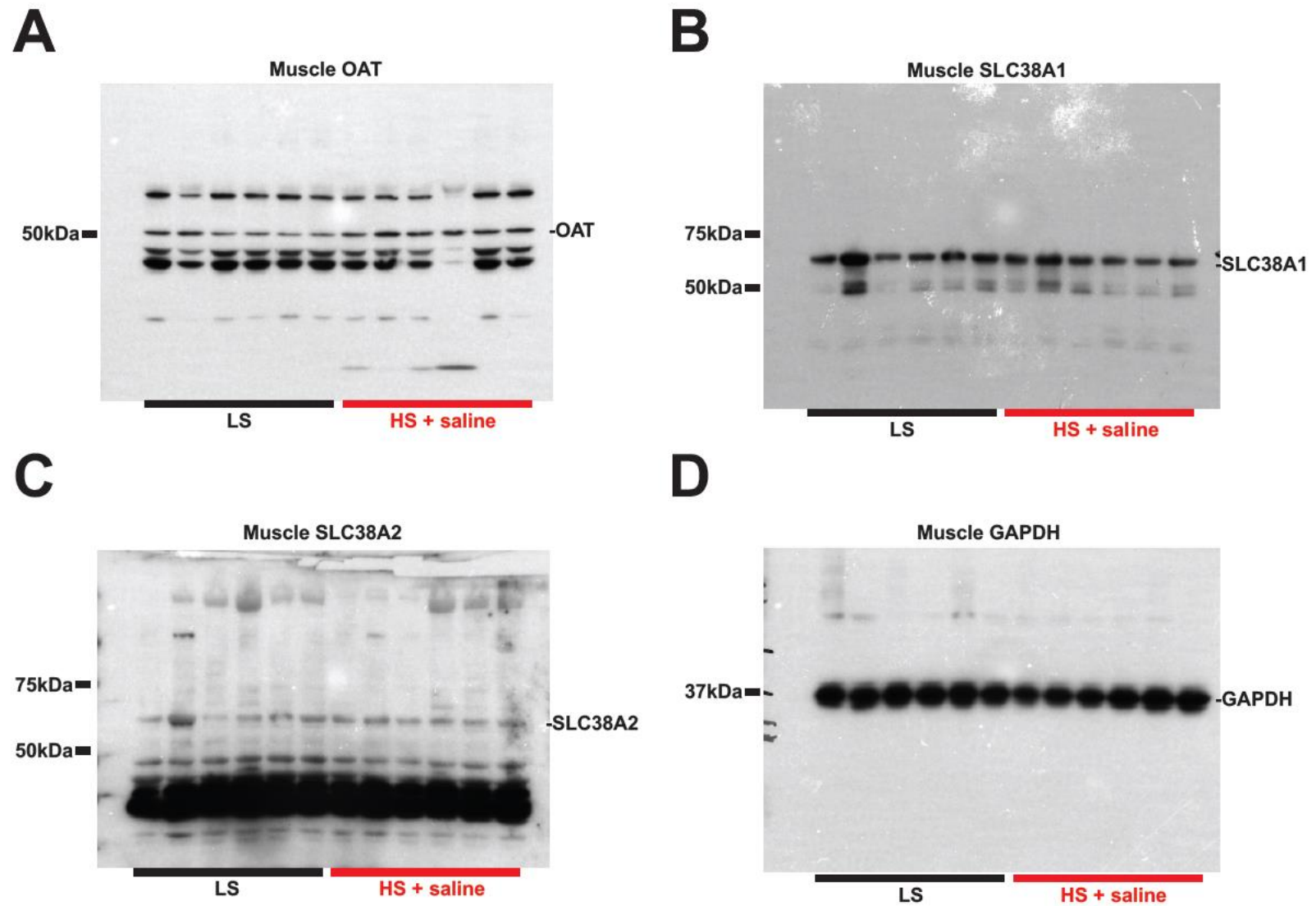
Online Supplemental Figure 7: Full western blots of Atg5, p62 and GAPDH expression in skeletal muscle of mice with low salt (LS; n=6) or high salt diet (HS+saline; n=6). *Panel A:* Atg5, *Panel B:* p62, *Panel C:* GAPDH expression. *Panel D:* Quantification of Atg5 and p62 protein relative to GAPDH protein expression, and metabolomic analysis of the change in 1-methyl histidine and 3-methyl histidine content in skeletal muscle of the mice.



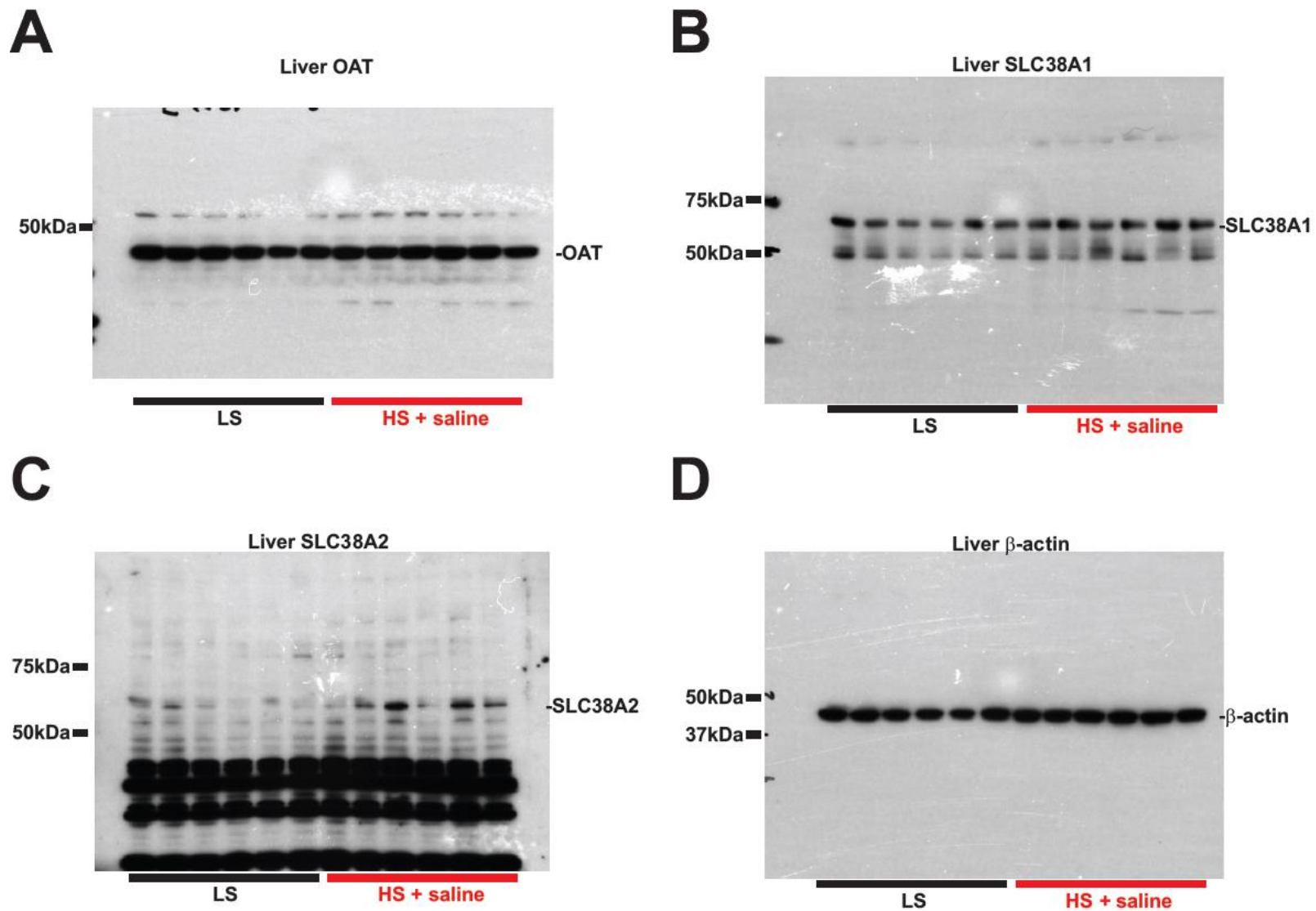
Online Supplemental Figure 8: Scheme of the deamination and the transamination route for nitrogen transfer of muscle amino acids into the liver urea cycle. Salt-induced changes in the metabolome are depicted in blue (decrease) or green (increase).



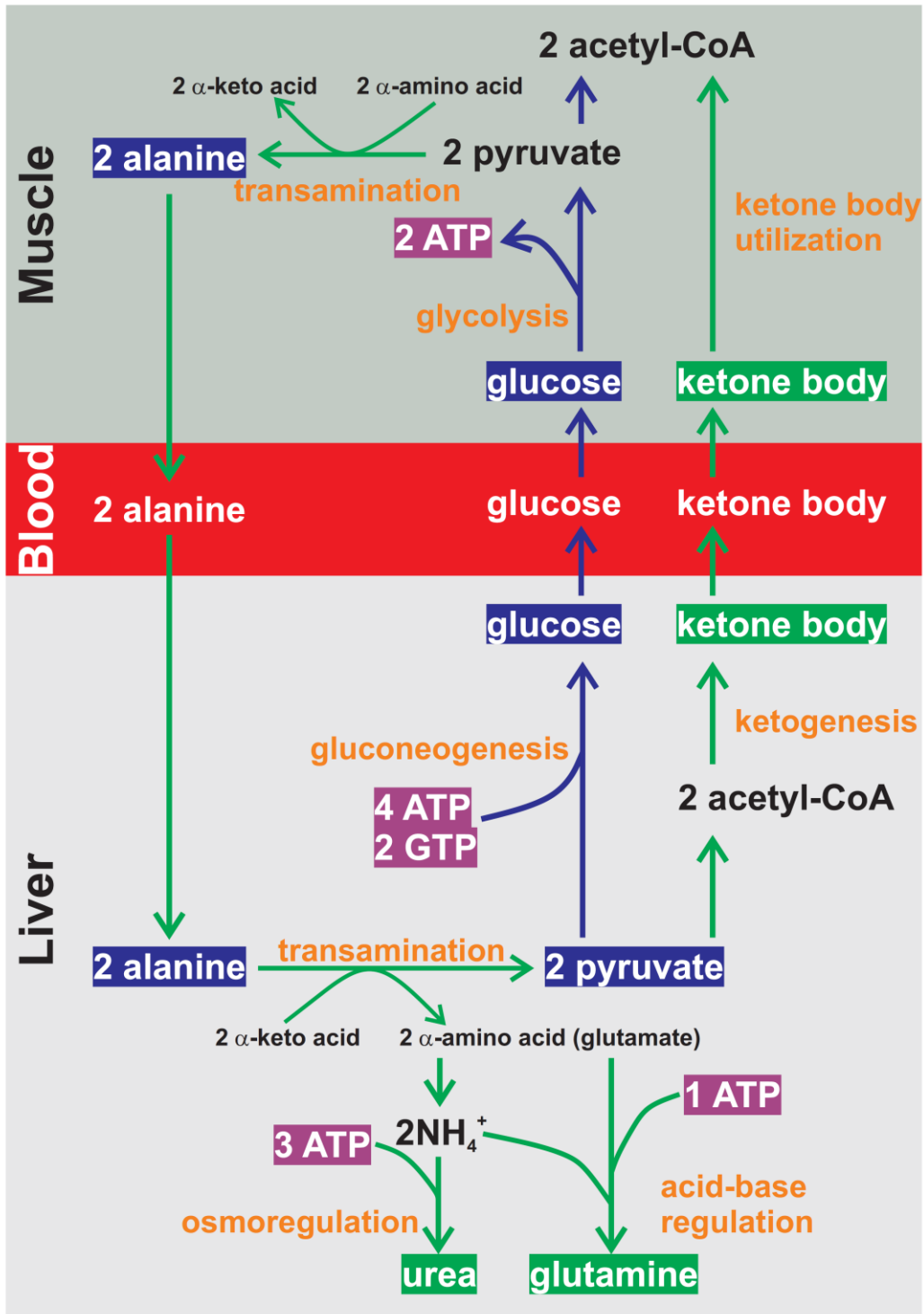
Online Supplemental Figure 9: Differences in energy metabolism, urea metabolism, and amino acid nitrogen transfer between muscle and liver. Salt-induced changes in the metabolome are depicted in blue (decrease) or green (increase). OAT: ornithine aminotransferase, ASL: argininosuccinate lyase.



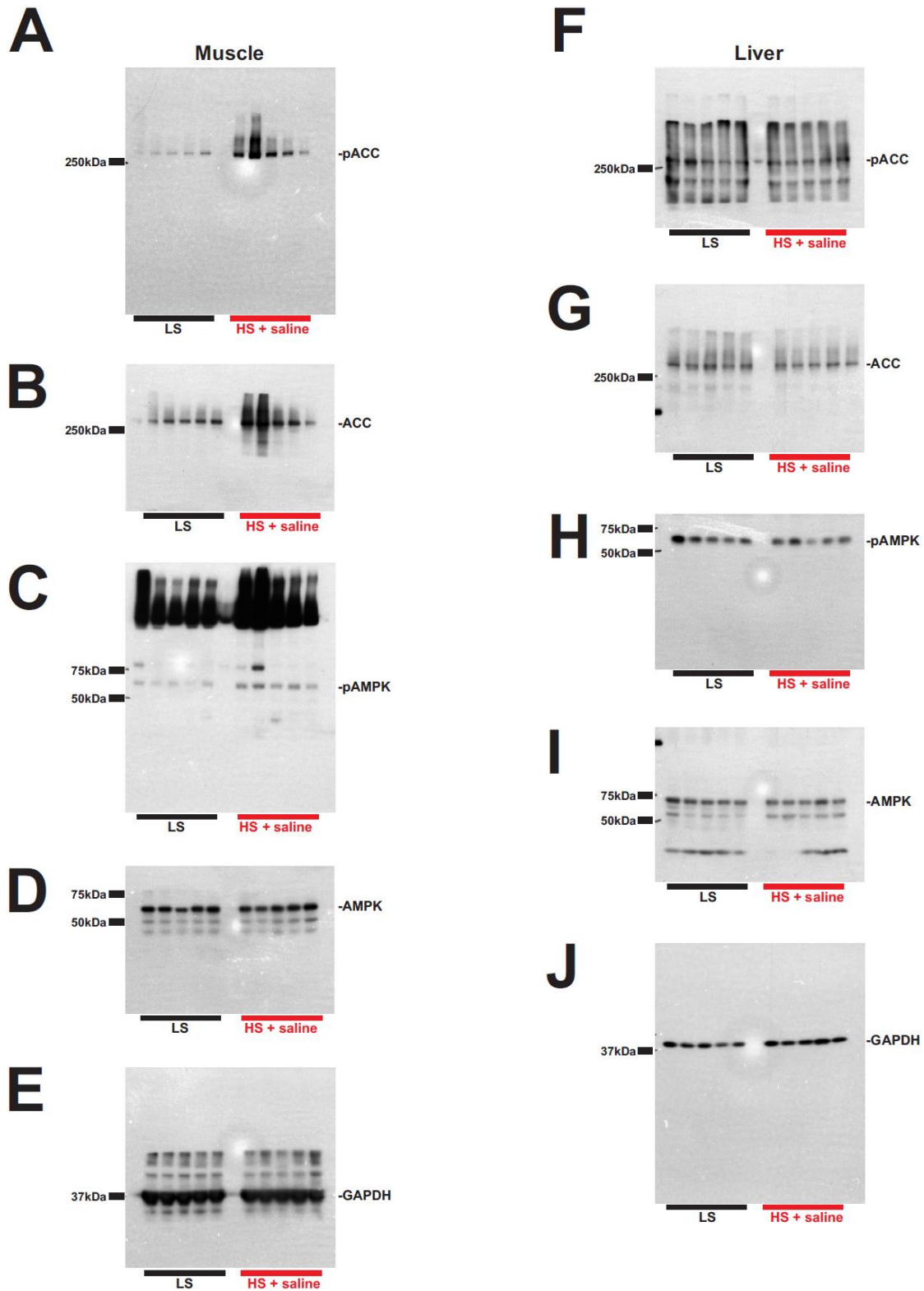
Online Supplemental Figure 10: Full western blots of ornithine aminotransferase, SLC38A1, SLC38A2, and GAPDH expression in skeletal muscle of mice with low salt (LS; n=6) or high salt diet (HS+saline; n=6).



Online Supplemental Figure 11: Full western blots of ornithine aminotransferase, SLC38A1, SLC38A2, and GAPDH expression in liver of mice with low salt (LS; n=6) or high salt diet (HS+saline; n=6).

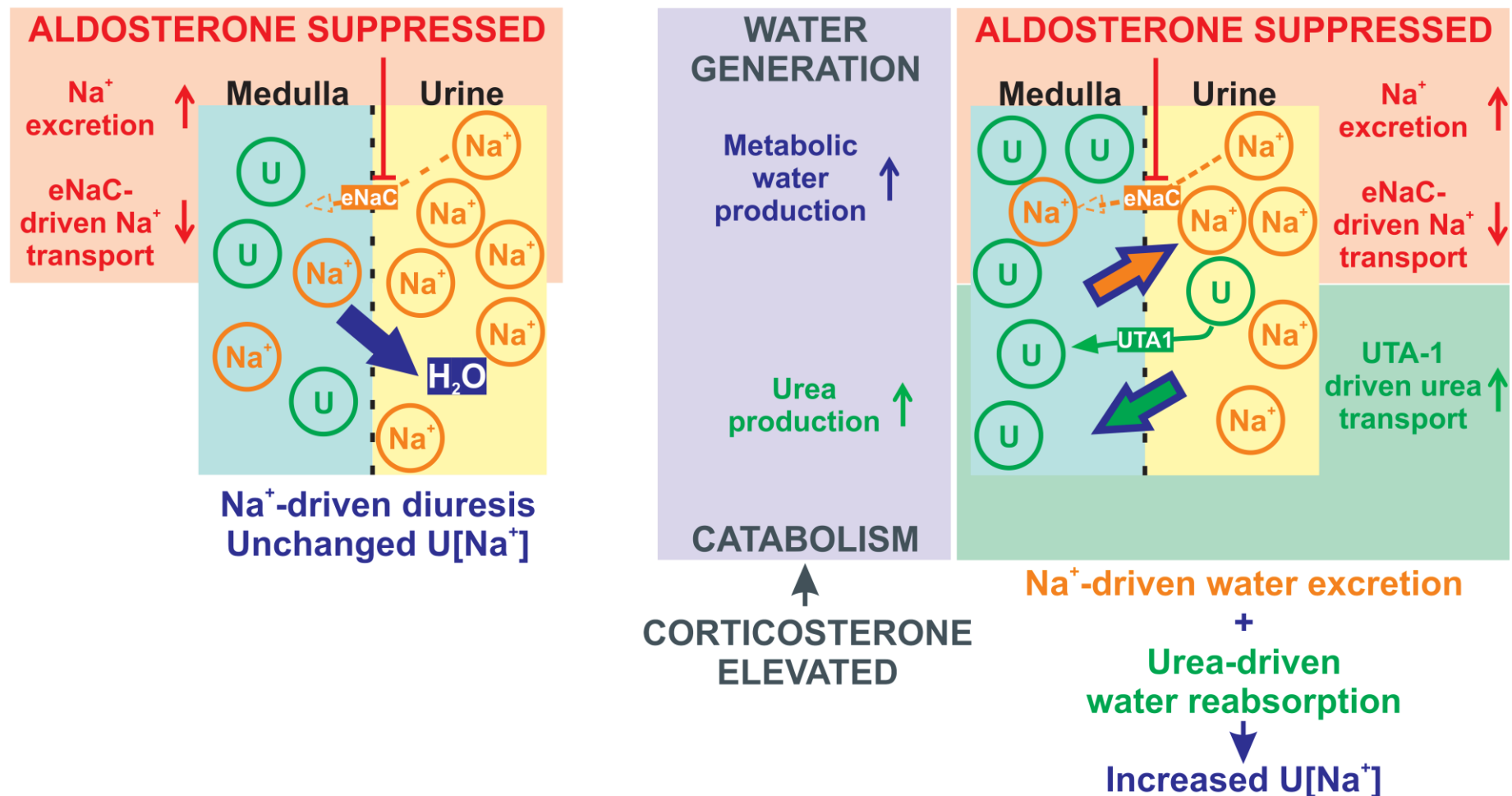


Online Supplemental Figure 12: Energetic consequences of nitrogen transfer from muscle to liver via the alanine-glucose-nitrogen shuttle in HS mice. Liver urea osmolyte and glutamine generation is energy intense. Regeneration of glucose from alanine via gluconeogenesis is an additional energy-intensive metabolic pathway. In the catabolic situation, liver prefers ketogenesis, because ketogenesis is energy-neutral and therefore energetically advantageous over gluconeogenesis. Reduction in gluconeogenesis contributes to low glucose levels in liver and in muscle. Salt-induced changes in the metabolomic pathways are depicted in blue (decrease) or green (increase).



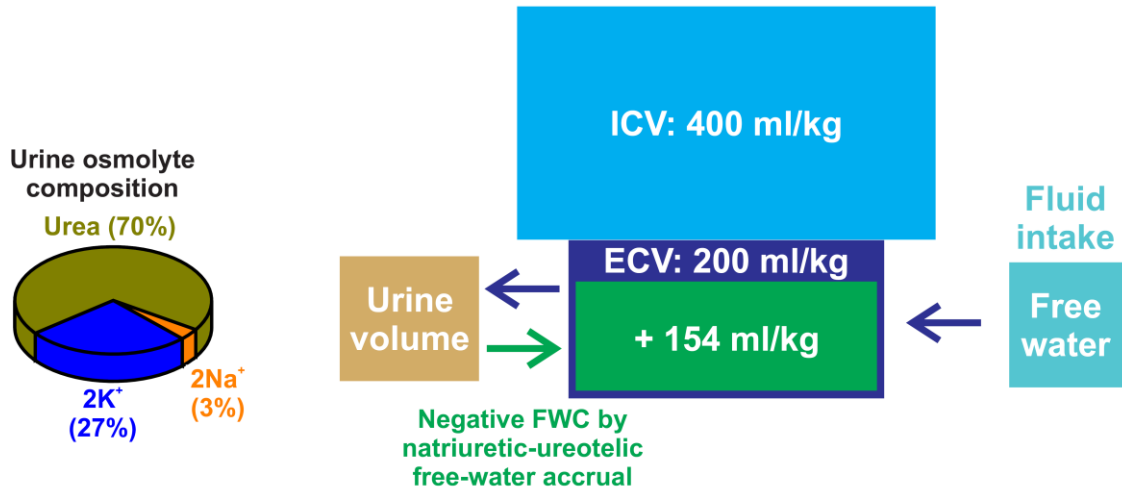
Online Supplemental Figure 13: Full western blots of ACC and AMPK protein expression in muscle and in liver of mice with low salt (LS; n=5) or high salt diet (HS+saline; n=5). *Panel A:* pACC in muscle, *Panel B:* ACC in muscle, *Panel C:* pAMPK in muscle, *Panel D:* AMPK in muscle, *Panel E:* GAPDH in muscle, *Panel F:* pACC in liver, *Panel G:* ACC in liver, *Panel H:* pAMPK in liver, *Panel I:* AMPK in liver, *Panel J:* GAPDH in liver.

A. Traditional natriuretic concept **B. Alternative natriuretic-ureotelic concept**

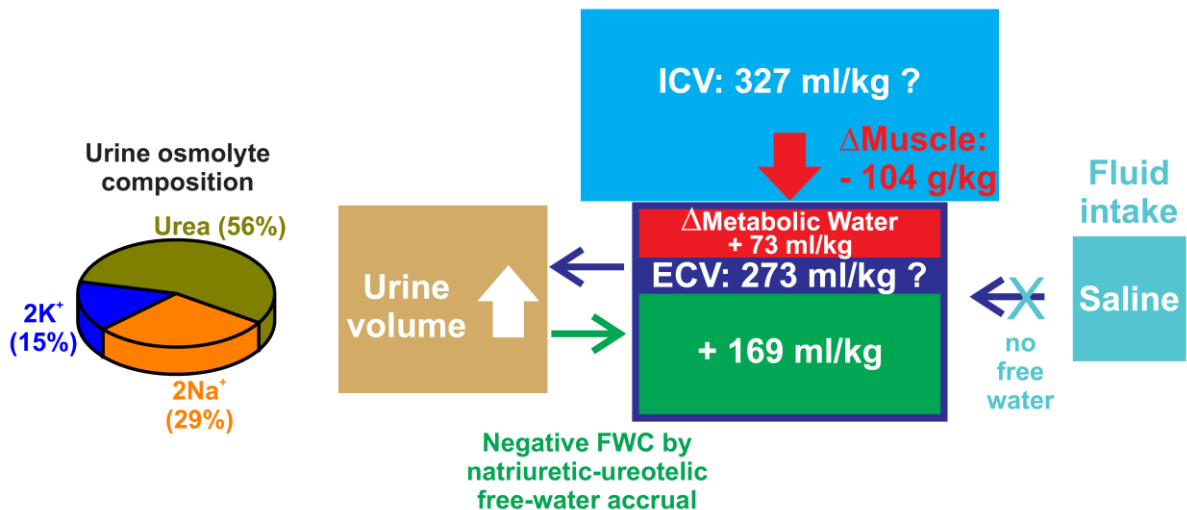


Online Supplemental Figure 14: Concept of natriuretic ureotelic regulation of salt and water metabolism. *Panel A.* Natriuretic concept: A high-salt diet suppresses aldosterone excretion, reduces eNaC activity, results in increased sodium excretion into the urine, which in turn induces osmotic diuresis. Natriuretic regulation thus predisposes to renal water loss. *Panel B.* Natriuretic-ureotelic concept: The sodium-induced water excretion is prevented by UTA1-driven increased urea transport, resulting in increased medullary urea osmolyte accumulation, which provides with the osmotic driving force necessary to maintain the renal concentration mechanism for body water conservation. The natriuretic-ureotelic osmolyte excretion pattern for renal water conservation occurs in HS+tap mice, in HS+saline mice, and in men with a 6 g/d increase in salt intake. Additional salt-driven increases in glucocorticoid levels were observed in the human study, and in HS+saline mice, in which we found a catabolic state with energy-intensive urea osmolyte production and increased metabolic water formation.

A. Low-salt diet group



B. High-salt diet + saline group



Online Supplemental Figure 15: Sources of endogenous water accrual in LS and HS+saline mice after pair feeding. Panel A. LS mice generated 154 ml/kg free water by separating surplus osmolytes from water by negative free-water clearance within the renal concentration process. This endogenous free water accrual corresponds to 75% of the estimated size of the extracellular volume. Osmolyte excretion is dominated by urea. Panel B. HS+saline mice maintained the renal concentration process by UTA1-driven urea accumulation, and generated 169 ml/kg free water by urine concentration. Osmolyte excretion was still dominated by urea, but the probability of Na⁺ and accompanying anion excretion was increased. Additional glucocorticoid-driven catabolism resulted in muscle wasting and translocation of 73 ml/kg water from the intracellular space into the extracellular space. It is unclear whether the resulting extracellular water surplus is excreted or retained in the body when body composition changes. ICV: intracellular volume. ECV: extracellular volume.

	<0.1% NaCl diet	4% NaCl diet
Energy content (kcal/g chow)	3.3	3.1
protein (% of wet weight)	19.3	19.4
protein (% of kcal intake)	23.7	24.7
carbohydrates (% of wet weight)	50.6	47.5
carbohydrates (% of kcal intake)	62	60.4
fat (% of wet weight)	5.2	5.2
fat (% of kcal intake)	14.3	14.9
Ingredients (in g/kg chow)		
	<0.1% NaCl diet	4% NaCl diet
Wheat	350	350
Corn	314.49	263.99
Soybean Meal (48%)	190	197
Corn Gluten Meal (60%)	50	52
Alfalfa Meal (17%), dehydrated	30	30
Corn oil	33	34.5
Dicalcium Phosphate, FG (18.5% P, 21% Ca)	14	14
Calcium Carbonate, FG (38%)	12	12
Mineral Mix, TSD (80318)	1.5	1.5
Vitamin Mix, TSD (81125)	3	3
DL-Methionine, FG (99%)	1	1
L-Lysine HCl, FG (78%)	1	1
Ethoxyquin, antioxidant	0.01	0.01
Sodium Chloride	0	40

Online Supplemental Table 1: Caloric content and ingredients in the low-salt and high-salt chow.